Journal of Electromagnetic Waves and Applications, 2013
Vol. 27, No. 17, 2155–2165, http://dx.doi.org/10.1080/09205071.2013.834274

Taylor & Francis
Taylor & Francis Group

Improved analysis of high-performances planar waveguide slot arrays

Giovanni Andrea Casula*, Giorgio Montisci, Giuseppe Mazzarella, Paolo Maxia and Alessandro Fanti

Dipartimento di Ingegneria Elettrica ed Elettronica, Università degli Studi di Cagliari, Piazza D'Armi, 09123 Cagliari, Italy

(*Received 17 June 2013; accepted 8 August 2013*)

An improved analysis procedure for planar waveguide slot arrays has been devised and assessed. It takes into account the main interferences between radiating and coupling slots, and between coupling slots and *T*-junctions, and waveguide bends used in the array feeding network. All these effects have been modeled using in-house MoM codes, and Elliott's slot array model has been extended to include them. The results of this improved procedure have been compared with experimental data showing a very good agreement.

Keywords: slot arrays; waveguide antennas; monopulse radar antennas; planar longitudinal slot arrays

1. Introduction

Planar arrays of longitudinal slots are very popular microwave antennas because of their high performance,[1,2] especially in the *X*-band and beyond.[3–5] Their most important advantages are the low loss, the high power they can carry, the polarization purity (either linear [6,7] or circular [8]), the high efficiency and gain, and good mechanical strength. For these reasons, planar slot arrays are frequently used as radar antennas, since they can also provide a very low-level of side lobes, so that the position of the object can be detected with the least possible ambiguity. As a matter of fact, high-performance Radars require Ultra-Low-Side Lobes antennas,[9] characterized by a Side Lobe Level (SLL) significantly lower than the typically required SLL. Therefore, for such antennas, an increase in the level of the near-in side lobes as small as 2 dB, or even an inaccurate prediction of their topography, can be unacceptable. This calls for an accurate characterization of planar waveguide slot arrays for high-performance applications.

The most accurate slot array model has been proposed by Elliott [6]. In this model, the slot excitation is related to both the waveguide mode voltage at the slot location and to the mutual coupling, but the Elliott model allows for an accurate analysis of the array only at the design frequency. In [10], the Elliott analysis procedure has been extended to compute the frequency response of a complete planar slot array, taking into account both the beam forming network and the frequency behavior of the slot couplers

*Corresponding author. Email: a.casula@diee.unica.it

used in the feeding network. However, the performance of waveguide slot arrays, both in terms of return loss and radiated field is influenced by several second-order effects in the feeding network,[11] such as the higher-order mode interaction between coupling slots,[12] the interaction between slot couplers and radiating slots,[13,14] and the interaction between slot couplers and waveguide bends.[15] Therefore, high-performance slot antennas require more sophisticated models than.[6,10] This is fundamental also to devise design procedures for slot arrays, either based on the Elliott model itself [2,16] or using random optimization techniques.[17–22]

In many radar applications, a waveguide slot array is divided into an appropriate number of sub-arrays (as that in [10] Figures 1 and 2), mainly to increase the frequency bandwidth. The main feeding point of each sub-array is usually realized using a *T*-junction, as in Figure 1, or sometimes using a rotated slot. Here we concentrate on the former, which is the most popular by far. Planar arrays fed by one or more *T*-junctions placed in the array *E*-plane are, in fact, quite common, especially for the implementation of monopulse arrays. In such arrays, the feeding guide must terminate with a shorted termination, half a wavelength beyond the last coupling slot, and this is usually realized with an "L" or "U" bend, which interacts with the coupling slot.[15] This configuration has been used, for example, in monopulse waveguide slot arrays of the GRIFO family by Selex Galileo [23]. In this case, the array feeding network must be considered non ideal, even in the first approximation.

The starting point of all analysis procedures for slot arrays is the Elliott analysis procedure,[2] extended to take into account the frequency behavior of both the radiating waveguide [24] and the feeding network.[10,25] From them many rigorous techniques have been proposed, aiming at evaluating different radiating structures [26–28] or to include second-order effects.[3,10,15,25,29,30] It is worth noting that this latter point is by no means straightforward. So, some important effects have been described (and evaluated) but not integrated into a complete analysis procedure. For the monopulse array described before, we must take into account:

(i) the strong interaction between the *T*-junction and the coupling slots connecting the feeding and radiating waveguide;
(ii) the interaction between the coupling slot and the nearby radiating slots;
(iii) the effect of the bent terminations.

As discussed in [26], the *T*-junction introduces a perturbation on the slots' excitations which can cause a rise in the first side lobes as large as 3 dB (and sometimes

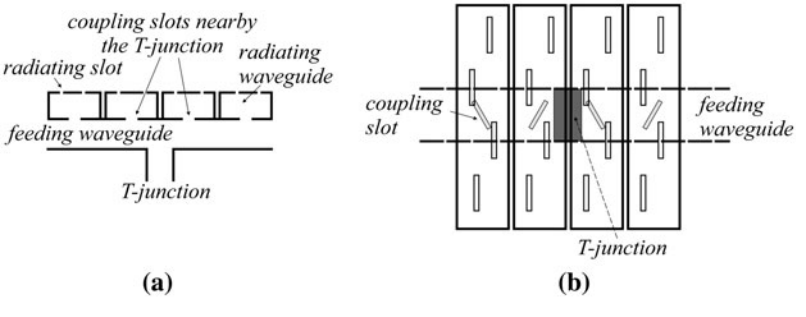

Figure 1. (a) Geometry of a sub-array with a feeding *T*-junction: side view; (b) Geometry of a sub-array with a feeding *T*-junction: top view.

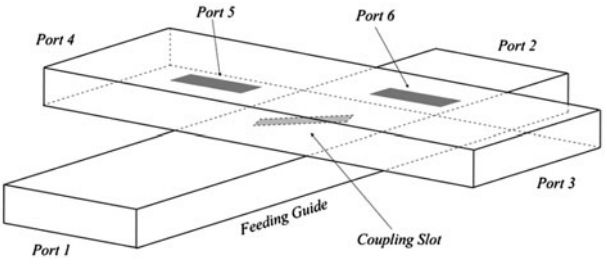

Figure 2. Inclined coupling slot and nearby radiating slots.

even beyond), if compared to the ideal case. However, even with this effect included, the simulated side-lobe topography can be very different from the actual one.

In this work, we show that a very good agreement between the simulated side-lobe (and, more generally, pattern) topography and the measured one can be obtained only if all three interference effects are taken into account for the analysis. In order to include (i)–(iii) into an analysis procedure, first a suitable model must be devised for the specific effect (the interaction between the coupling slot and the nearby radiating slots, or the effect of the bent terminations in our case), for example by using an appropriate matrix model (an hybrid matrix in our case), and then the equations used to devise this model must be appropriately inserted into the equations describing the arrays' behavior.[10]

The results of our model have been compared with experimental data, showing a very good agreement.

2. Array model

In this section we describe how the analysis procedure, first proposed in [10] and then improved in [26], has been further extended in order to take into account the interaction between the coupling slots (feeding the radiating waveguides of the array) and both the nearby radiating slots (Figure 1(b)), and the waveguide bends. Therefore, for the sake of simplicity and as matter of coherence, and so as to ease the discussion, all the symbols and variables used in this paper are the same as in [10], and we will also refer to some figures and equations presented in [10]. Following Elliott [6], the radiating part of a waveguide slot array can be modeled using two sets of equations ([6], Equations (10), (33)), which express the slot voltages V^S_n as a function of both the active slot admittances Y^S_n and of the mode voltages V_n (in the radiating guide) at the position of each slot. The model of a feeding waveguide is shown in ([10], Figure 3), where the array is directly fed from one side by the current I_A. We call this kind of feeding an "ideal feeding", since in this case the feeding port does not interact with the slot couplers. The analysis of the waveguide slot array, fed by an ideal feeding amounts to the solution of the linear system built by:

(1) the equations linking currents and voltages on the feeding waveguide ([10], Equations (10.a), (10.b));
(2) the equations related to the mode voltages in the radiating waveguides ([10], Equation (3)), taking into account that, for non-resonant spacing, the mode voltage distribution depends on the active admittances of all the slots of the array;
(3) the two Elliott's design equations describing the behavior of the radiating slots in the radiating waveguides ([10], Equations (1.a) and (1.b)).

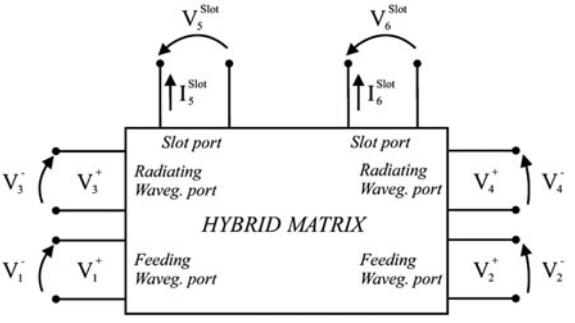

Figure 3. 6-Port matrix modeling the interferences between the inclined coupling slot and the two nearby radiating slots.

Actual feeding usually employs a *T*-junction, as in Figure 1. The interaction of this *T*-junction with the coupling slots cannot be underestimated, as discussed in [26]. However, as we will demonstrate here, the interaction between the feeding slot couplers and the nearest radiating slots is equally important in order to design arrays with very stringent requirements. In order to include its effect in the analysis model, we represent the portion of the array, composed of the slot coupler and its nearest radiating slots, together with the appropriate portion of the feeding and radiating waveguides (Figure 2), as a six-port network (Figure 3).

As listed in Figure 2, ports 1–4 are standard (namely, TE_{10}-mode) waveguide ports, whereas ports 5 and 6 are "slot" ports, where the slot voltage, defined in ([6], Equation (10)), and widely used to describe the slot array aperture distribution, is the main quantity. Since the ports are of different kinds, we use a hybrid representation for the network matrix. More precisely, we use, as port quantities, the incident and scattered wave amplitudes for ports 1–4 (the waveguide ports), and the total currents and voltages for ports 5–6 (the slot ports). The Hybrid matrix corresponding to the six-port network in Figure 3 is therefore:

$$\begin{aligned}
V_1^- &= S_{11}V_1^+ + S_{12}V_2^+ + S_{13}V_3^+ + S_{14}V_4^+ + B_{15}I_5^{\text{Slot}} + B_{16}I_6^{\text{Slot}} \\
V_2^- &= S_{21}V_1^+ + S_{22}V_2^+ + S_{23}V_3^+ + S_{24}V_4^+ + B_{25}I_5^{\text{Slot}} + B_{26}I_6^{\text{Slot}} \\
V_3^- &= S_{31}V_1^+ + S_{32}V_2^+ + S_{33}V_3^+ + S_{34}V_4^+ + B_{35}I_5^{\text{Slot}} + B_{36}I_6^{\text{Slot}} \\
V_4^- &= S_{41}V_1^+ + S_{42}V_2^+ + S_{43}V_3^+ + S_{44}V_4^+ + B_{45}I_5^{\text{Slot}} + B_{46}I_6^{\text{Slot}} \\
V_5^{\text{Slot}} &= A_{51}V_1^+ + A_{52}V_2^+ + A_{53}V_3^+ + A_{54}V_4^+ + Z_{55}I_5^{\text{Slot}} + Z_{56}I_6^{\text{Slot}} \\
V_6^{\text{Slot}} &= A_{61}V_1^+ + A_{62}V_2^+ + A_{63}V_3^+ + A_{64}V_4^+ + Z_{65}I_5^{\text{Slot}} + Z_{66}I_6^{\text{Slot}}
\end{aligned} \tag{1}$$

where in B_{ij} and Z_{ij} are impedances, and A_{ij} and S_{ij} are adimensional coefficients. All the 6×6 matrix coefficients of Equations (1) have been computed using an in-house MoM procedure for the analysis of the structure depicted in Figure 2. The reader is addressed to [15,31] for further details about this procedure. Equations (1) have been suitably integrated in the analysis model presented in [26]. The effect of the bent waveguide terminations has also been included in the array analysis using the model described in [15]. The resulting linear system allows to analyze the array taking into account all three effects (i) – (iii) listed in the Introduction section. Starting from the linear system described in [10], formed by Equations (1.a), (1.b), (3), (10.a), (10.b), and the one between (11.a) and (11.

b) (depending on the source model), each of the effects (i) – (iii) can be taken into account by adding further equations to the linear system. In particular:

(1) the inclusion of the interaction between each *T*-junction and the nearby coupling slots connecting the feeding and radiating waveguide requires five new equations (Equation (1) of [26]) to be added to the linear system, describing the *T*-junction as a five-port network. The five new unknowns we must add to the system are, referring to Equation (1) of [26]: V_{AT} (or I_{AT} depending on the source model), I_{L_SX}, I_{L_DX}, $I^{C}{}_{SX}$, and $I^{C}{}_{DX}$. Therefore, for an array with N_T *T*-junctions we have to add $5^{*}N_T$ new equations, and $5^{*}N_T$ unknowns to the linear system of [10].
(2) the inclusion of the interaction between each coupling slot and the nearby radiating slots requires six new equations (Equation (1)) to be added to the linear system, describing the interaction between the feeding slot couplers and the nearest radiating slots as a six-port network. The 6 new unknowns we must add to the system are referring to Equation (1): $V_1^-, V_2^-, V_3^-, V_4^-, V_5^{\mathrm{Slot}}$ and V_6^{Slot}. Therefore, for an array with N_C couplers, we have to add $6^{*}N_C$ new equations, and $6^{*}N_C$ unknowns to the linear system of [10].
(3) the inclusion of the effect of each bent termination requires 2 new equations ([15]) to be added to the linear system, describing the bent termination as a two-port network. The two new unknowns we must add to the system are, referring to [15]: $V^{SB}{}_1, V^{SB}{}_2$, representing respectively the voltage at port 1 and at port two of the two-port network modeling the bend termination. Therefore, for an array with N_B bent terminations, we have to add $2^{*}N_B$ new equations, and $2^{*}N_B$ unknowns to the linear system of [10].

3. Results and discussion

The improved array analysis procedure described above has been tested on several planar arrays with different configurations and architectures (symmetric or asymmetric, balanced or unbalanced, uniform or non-uniform, with or without sub-array architecture). We have found that all the effects included in our improved model are significant only when the array, or the sub-array, has an asymmetric or unbalanced configuration, and when the required side lobe level is low enough (namely, below −20 dB). However, the four sub-arrays of all monopulse radar slot arrays are asymmetric, and usually such arrays also require very low SLL,[9] so that they belong to this group.[23,32,33] On the other hand, for symmetric configurations, these effects have a marginal repercussion on the array behavior, since the array symmetry almost compensates them.

The first two examples shown in this section are referred to an asymmetric and unbalanced array with 24 radiating waveguides, each one with six radiating slots (Figure 4). This array is divided into two sub-arrays, each one fed by a feeding waveguide, which is in turn fed by a *T*-junction. The *T*-junction is placed between the 8th and the 9th radiating guide in the sub-array 1, and between the 4th and the 5th radiating guide in the sub-array 2 (the array structure is therefore 8-4, 4-8). These arrays have been designed with a synthesis procedure based on Elliott's model [6,16] at the operating frequency of 9 GHz, requiring two different aperture distributions, namely a Taylor pattern with −25 dB side-lobes (array 1) and a Chebycheff pattern with −25 dB

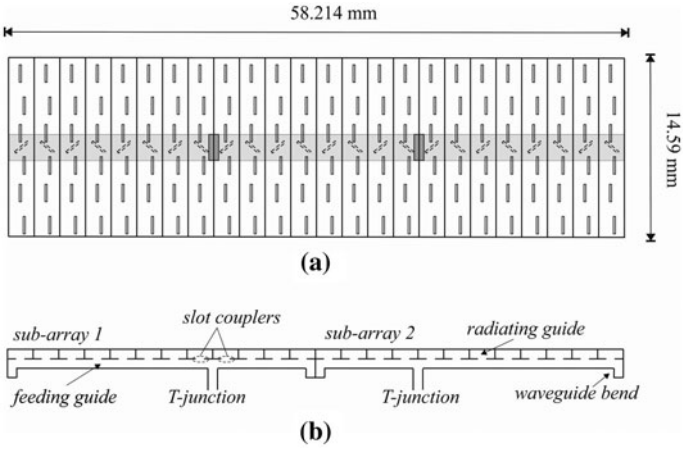

Figure 4. Geometry of the 24 × 6 planar array: (a) top view; (b) sectional view.

side-lobes (array 2) for the *E*-plane. A uniform pattern in the *H*-plane has been required in both cases. For these two test cases, the model presented in this paper has been assessed by comparison with the results of Ansys HFSS.

In Figures 5 and 6, the radiation patterns in the *E*-plane are reported for the two-designed arrays. The range is limited to ±30° in order to highlight the interferences effects. Both cases have been analysed including only the effect of the *T*-junction, and using the complete improved model described in this work, taking into account also the interaction between the coupling slots and the nearby radiating slots and the effect of the bent terminations.

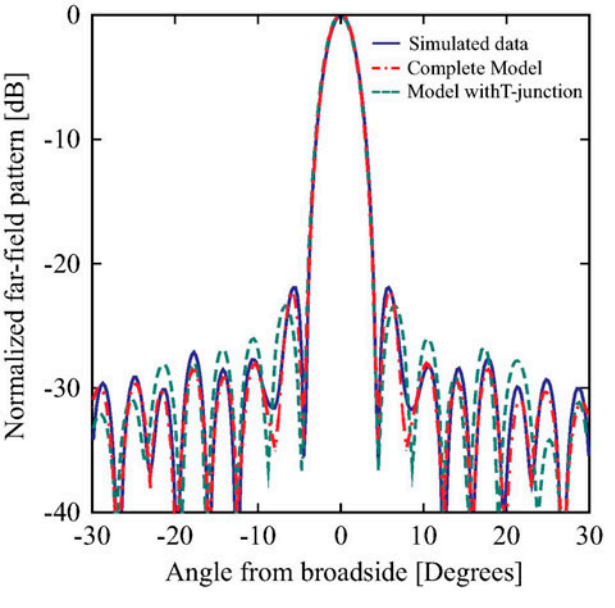

Figure 5. *E*-plane radiation pattern of the 24 × 6 planar array with a 25 dB Taylor distribution.

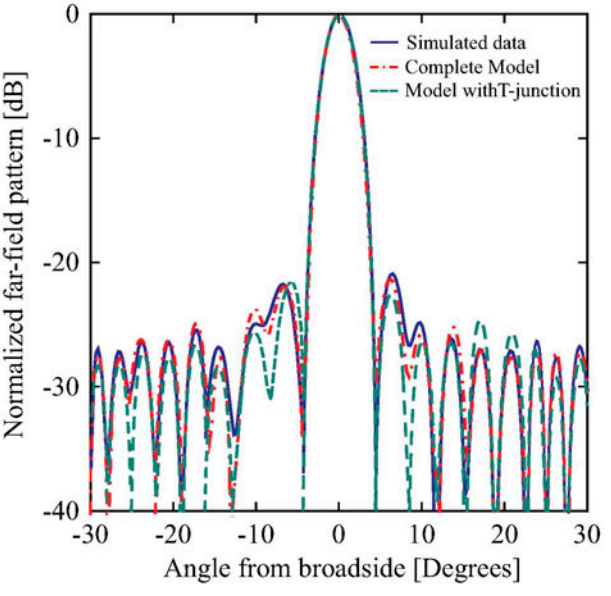

Figure 6. *E*-plane radiation pattern of the 24×6 planar array with a 25 dB Chebycheff distribution.

The results shown in Figures 5 and 6, confirm that the prediction of the model taking into account only the effect of the *T*-junctions can sometimes be acceptable, while using the improved analysis model the prediction of the array behavior is significantly closer to the simulated data. The deterioration of the far-field caused by the second-order effects described here (*T*-junction, slot couplers, short bends) cannot be neglected, since they produce an increase of about 5 dB of the SLL. Inclusion of the *T*-junction alone (as in [26]) reduces the deterioration to about 3 dB.

The last reported example, which will be described in more detail, is an *X*-Band monopulse array with a diameter equal to 72 cm, and whose geometry is depicted in Figure 7. The array has been designed with a synthesis procedure based on Elliott's model,[6] and its prototype has been manufactured and measured by Selex Galileo. This array consists of 56 radiating waveguides, each one with a different number of slots, and is divided into four sub-arrays. The array carries a total number of 656 radiating slots, and its beam forming network has 56 inclined coupling slots. Each sub-array is fed by a feeding waveguide, fed in turn by a *T*-junction, and each feeding waveguide ends with two-shorted bends,[15] one for each side, as indicated in Figure 7. Hence, there are a total of 8 shorted bends in the beam forming network of the array. The position of the *T*-junctions is between the 9th and the10th radiating guide for sub-arrays 1 and 2, and between the 5th and the 6th radiating guide for sub-arrays 3 and 4, with an array structure (9-5, 5-9, 9-5, 5-9). This array has been designed to radiate a Taylor pattern with -30 dB side-lobes both in the *E*-plane and in the *H*-plane. The results presented in this section will be used both to assess our analysis model, and to show the relevance of the proposed improvement. In order to assess the improved model, we have compared, for two different lengths of the bent short circuits, the measured far-field pattern with the results of our analysis procedure, which includes all three effects listed in Section I. Figure 8 shows the comparison between the measured and

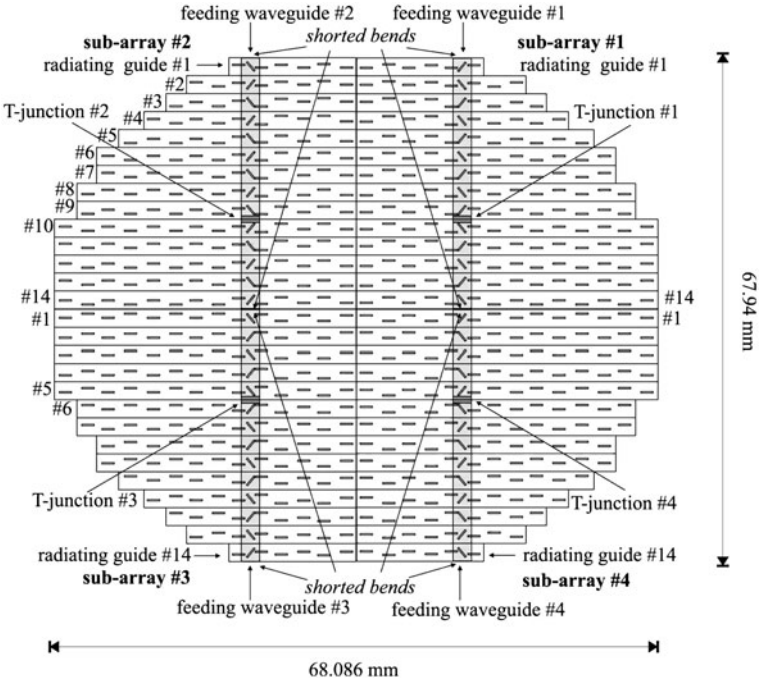

Figure 7. Geometry of the monopulse planar array.

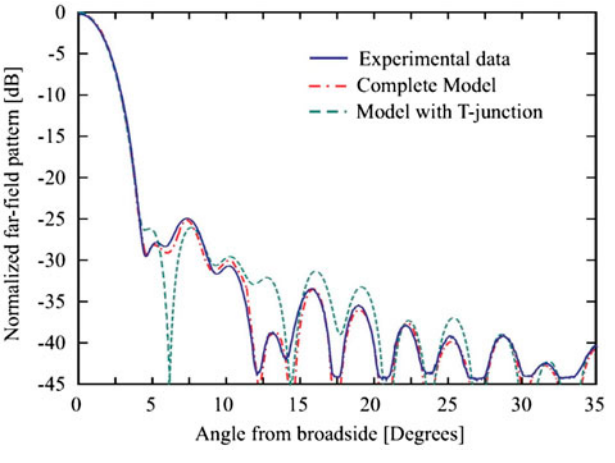

Figure 8. Far-field pattern in the *E*-plane of the array in Figure 7 with the short bends length equal to 9.9 mm. The analysis model with the *T*-junction has been done using a straight shorted termination for the feeding waveguides with an impedance of 0 Ω.

the computed *E*-plane radiation pattern using the improved analysis model, for the array with the 8 shorted bends having a length of 9.9 mm. This length corresponds to an equivalent input impedance of the shorted bends equal to a short circuit (0 Ω). In Figure 9, the same comparison is reported when the 8 shorted bends have a length of 12.4 mm, which corresponds to an equivalent input impedance of the shorted bends

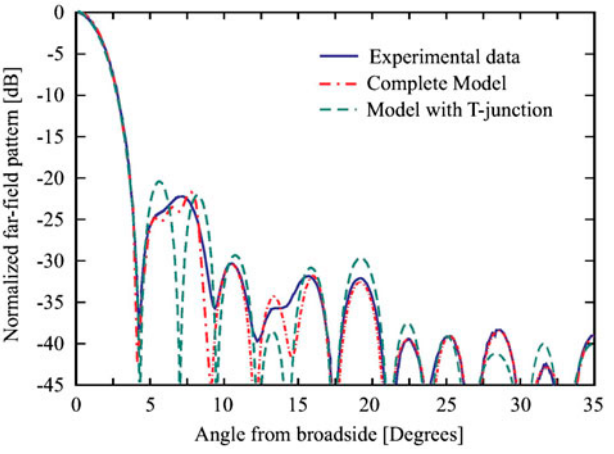

Figure 9. Far-field pattern in the *E*-plane of the array in Figure 7 with the short bends length equal to 12.4 mm. The analysis model with the *T*-junction has been done using a straight shorted termination for the feeding waveguides with an impedance of 200 Ω.

equal to 0 + j 200 Ω. The range is limited to [0°, 35°] in order to highlight the interferences effects.

Then, both the cases have been also analyzed including only the effect of the *T*-junction, and the comparison with the measurement has been reported in Figures 8 and 9. In both cases, the analysis has been done using a straight-shorted termination for the feeding waveguides. From the data shown in Figures 8 and 9, it is apparent that the prediction of the model, taking into account only the effect of the *T*-junctions, is not satisfactory. On the other hand, the array behavior is very accurately predicted by the improved analysis model, which is significantly closer to the experimental data.

For the arrays under test, we have found that the effect of the interferences between the coupler, the bent terminations and the nearby radiating slots, consists of a variation around 2% of the excitation amplitude of these radiating slots, and a variation of the excitation phase of 5°–10°, compared to the "ideal" case. As we can see in Figures 5 and 6, this effect on the slot excitations causes an important variation of the first side lobes. The degradation on the far-field pattern is significant only in the array *E*-plane, whereas the *H*-plane is not affected by the interaction between the coupling and radiating slots, showing only a negligible variation on the side lobes. Therefore, the *H*-plane-radiated fields have not been reported here.

4. Conclusion

An improved analysis procedure for planar waveguide slot arrays has been devised, taking into account both the effect of the feeding *T*-junction and the interaction between the slot couplers and the nearest radiating slots on one side and the waveguide bends on the other one. These effects cause a significant elevation of the first side lobes with respect to an ideal case [6,10] (up to 5–6 dB for the example considered in this paper), with an important degradation of the array behavior. Therefore, these effects cannot be neglected in the design of high-performance waveguide slot arrays, such as arrays with a very low SLL. The analysis model presented in this paper has been assessed by comparison with experimental data on a prototype realized by Selex Galileo.

Acknowledgments

Paolo Maxia gratefully acknowledges Sardinia Regional Government for the financial support of her PhD scholarship (P.O.R. Sardegna F.S.E. Operational Programme of the Autonomous Region of Sardinia, European Social Fund 2007–2013 – Axis IV Human Resources, Objective l.3, Line of Activity l.3.1.).

Alessandro Fanti gratefully acknowledges Sardinia Regional Government for the financial support of her Post Doc fellowship (P.O.R. Sardegna F.S.E. Operational Programme of the Autonomous Region of Sardinia, European Social Fund 2007–2013 – Axis IV Human Resources, Objective l.3, Line of Activity l.3.1.).

References

[1] Lo YT, Lee SW. Antenna handbook vol. 3: antenna applications. New York: Chapman and Hall; 1993.
[2] Elliot RS. Antenna theory and design. New York: Prentice-Hall; 1981.
[3] Rengarajan SR, Zawadzki MS, Hodges RE. Waveguide-slot array antenna design for low-average-sidelobe specifications. IEEE Antennas Propag. Mag. 2010;52:89–98.
[4] Casula GA, Montisci G. Design of dielectric-covered planar arrays of longitudinal slots. IEEE Antennas Wirel. Propag. Lett. 2009;8:752–755.
[5] Miura Y, Hirokawa J, Ando M, Shibuya Y, Yoshida G. Double-layer full-corporate-feed hollow-waveguide slot Ar-ray antenna in the 60-GHz band. IEEE Trans. Antennas Propagat. 2011;8:2844–2851.
[6] Elliot RS. An improved design procedure for small arrays of shunt slots. IEEE Trans. Antennas Propagat. 1983;31:48–53.
[7] Rengarajan SR. Compound radiating slot in a broad wall of a rectangular waveguide. IEEE Trans. Antennas Propagat. 1989;37:1116–1124.
[8] Montisci G. Design of circularly polarized waveguide slot linear arrays. IEEE Trans. Antennas Propag. 2006;54:3025–3029.
[9] Schrank H. Low sidelobe phased array antennas. IEEE Antennas Propag. Soc. Newsletter. 1983;25:4–9.
[10] Casula GA, Mazzarella G. A direct computation of the frequency response of planar waveguide slot arrays. IEEE Trans. Antennas Propag. 2004;52:1909–1912.
[11] Rengarajan SR, Josefsson LG, Elliott RS. Waveguide-fed slot antennas and arrays: a review. Electromagnetics. 1999;19:3–22.
[12] Rengarajan SR. An optimization procedure for including the higher order mode coupling between coupling slots in the design of a planar slot array. IEEE Antennas Wirel. Propag. Lett. 2008;7:785–787.
[13] Rengarajan SR, Shaw GM. Accurate characterization of coupling junctions in waveguide-fed planar slot arrays. IEEE Trans. Microwave Theory Tech. 1994;42:2239–2247.
[14] Mazzarella G, Montisci G. Accurate modeling of coupling junctions in dielectric covered waveguide slot arrays. Prog. Electromagnet. Res. M 2011;17:59–71.
[15] Mazzarella G, Montisci G. Accurate characterization of the interaction between coupling slots and waveguide bends in waveguide slot arrays. IEEE Trans. Microwave Theory Tech. 2000;48:1154–1157.
[16] Casula GA, Mazzarella G, Montisci G. Design of shaped beam planar arrays of waveguide longitudinal slots. Int. J. Antennas Propag. 2013;2013: 12 pp.
[17] Ares F, Villanueva E, Rodriguez JA, Rengarajan SR. Application of genetic algorithms in the design and optimization of array patterns. Int. Symp. Antennas Propag. 1997;3:1684–1687.
[18] Pazoki R, Rashed-Mohassel J. Bandwidth enhancement of resonant slot array antennas. J. Electromagnet. Waves App. 2007;21:1177–1189.
[19] Zhang Y, Li J-Y, Liang C-H, Xie Y-J. A fast analysis of large finite-slot phased arrays fed by rectangular waveguides. J. Electromagnet. Waves App. 2004;18:715–727.
[20] Zhao XW, Dang XJ, Zhang Y, Liang CH. MLFMA analysis of waveguide arrays with narrow-wall slots. J. Electromagnet. Waves App. 2007;21:1063–1078.
[21] Li J-Y, Li L-W, Gan Y-B. Method of moments analysis of waveguide slot antennas using the EFIE. J. Electromagnet. Waves App. 2005;19:1729–1748.

[22] Nie X-C, Gan Y-B, Yuan N, Wang C-F, Li L-W. An efficient hybrid method for analysis of slot arrays enclosed by a large radome. J. Electromagnet. Waves App. 2006;20:249–264.
[23] http://www.selexgalileo.com/SelexGalileo/EN/Business/Products/Radar
[24] Hamadallah M. Frequency limitations on broad-band performance of shunt slot arrays. IEEE Trans. Antennas Propag. 1989;37:817–823.
[25] Rengarajan SR, Chatterjee S. An investigation of bandwidth characteristics of waveguide-fed planar slot arrays. Electromagnetics. 2009;29:515–521.
[26] Casula GA, Mazzarella G, Montisci G. Effect of the feeding *T*-junctions in the performance of planar waveguide slot arrays. IEEE Antennas Wirel. Propag. Lett. 2012;11:953–956.
[27] Montisci G, Mazzarella G, Casula GA. Effective analysis of a waveguide longitudinal slot with cavity. IEEE Trans. Antennas Propagat. 2012;60:3104–3110.
[28] Tomura T, Hirokawa J, Hirano T, Ando M. Analysis of an X-shaped cavity-backed slot 2×2-element sub-array by hybrid MoM/FEM with numerical eigenmode basis functions. Int. Symp. Antennas Propag. 2012;1–2.
[29] Enneking A, Beyer R, Arndt F. Rigorous analysis of large finite waveguide-fed slot arrays including mutual internal and external higher-order mode coupling. Int. Symp. Antennas Propag. 2000;1:74–77.
[30] Kakatkar SS, Ray KP. Evaluation of mutual coupling between slots from dipole expressions. Prog. Electromagnet. Res. M 2009;9:123–138.
[31] Mazzarella G, Montisci G. Rigorous analysis of dielectric-covered narrow longitudinal shunt slots with finite wall thickness. Electromagnetics. 1999;19:407–418.
[32] Casula GA, Collu F, Mazzarella G. Effect of the beam forming network on the behavior of broadband planar waveguide slot arrays. Int. Symp. Antennas Propag. 2008;1–4.
[33] Sherman SM. Monopulse principles and techniques. Norwood (MA): Artech House; 1984.